Journal of Immunological Methods 472 (2019) 25–34

Contents lists available at ScienceDirect

Journal of Immunological Methods

journal homepage: www.elsevier.com/locate/jim

Optimisation of multiplex immunofluorescence for a non-spectral fluorescence scanning system

Chidozie C. Anyaegbu[a,b,1], Tracey F. Lee-Pullen[a,b,*,1], Timothy J. Miller[a,b], Tamara N. Abel[c], Cameron F. Platell[a,b], Melanie J. McCoy[a,b]

[a] St John of God Subiaco Hospital, PO Box 14, Subiaco, WA 6904, Australia
[b] Medical School, University of Western Australia, M507, 35 Stirling Highway, Crawley, WA 6009, Australia
[c] Telethon Kids Institute, University of Western Australia, Perth Children's Hospital, 15 Hospital Avenue, Nedlands, WA 6009, Australia

ARTICLE INFO

Keywords:
Fluorescence microscopy
Imaging
Immunohistochemistry
T cells
Colorectal

ABSTRACT

The use of multi-colour immunofluorescence (IF) for immunophenotyping in formalin-fixed paraffin-embedded tissue sections is gaining popularity worldwide. This technique allows for the simultaneous detection of multiple markers on the same tissue section, thereby yielding more complex information than is possible by chromogenic immunohistochemistry (IHC). However, many commercially-available multiplex IF kits are designed for use in conjunction with a multispectral imaging system, to which many research groups have limited access. Here we present two 5-colour IF panels designed for T cell characterisation in human colorectal tissue, which can be imaged using a non-spectral fluorescence slide scanner with standard band-pass filters. We describe the optimisation process and the key considerations in developing a multiplex fluorescence assay, and discuss some of the advantages and disadvantages of using multiplex IF with a non-spectral imaging system.

1. Introduction

In recent years, it has become evident that the type, density and/or spatial distribution of immune cells in tumour specimens is potentially valuable for predicting cancer prognosis and response to treatment (Schnell et al., 2018). In colorectal cancer, tumour-infiltrating T cell density can add important prognostic information over traditional pathological staging (Mlecnik et al., 2011) and efforts are underway to standardise T cell assessment for inclusion in routine pathology review (Galon et al., 2014; Pages et al., 2018). However, chromogenic immunohistochemistry (IHC), the gold standard in pathology for analysing proteins in tissues, can only assess one or two markers concurrently and is therefore unlikely to yield sufficiently detailed insights into complex interactions between multiple cells. This has driven the development of different multiplexed technologies that allow for simultaneous assessment of multiple markers on the same tissue section (Parra et al., 2019).

Multiplex immunofluorescence (IF) staining techniques using tyramide-signal amplification (TSA) are gaining popularity worldwide, as they allow researchers to use primary antibodies from the same species and thereby select antibodies solely on the basis of their performance (Stack et al., 2014; Blom et al., 2017; Feng et al., 2017; Parra et al., 2017; Gorris et al., 2018). Traditionally, multiplex IF or IHC has relied on using primary antibodies raised in different species to avoid cross-reactivity on application of fluorescently-labelled secondary antibodies (van der van der Loos, 2008). The range of host species in which commercially-available primary antibodies are produced therefore limits the value of this technique (most anti-human antibodies being raised in mouse, rabbit or goat). Multiplex IF using TSA involves sequential staining and stripping steps whereby deposited fluorophores remain on the tissue surface but antibody complexes are removed, allowing for the use of multiple primary antibodies raised in the same species in a single staining panel (Toth and Mezey, 2007; Zhang et al., 2017; Buchwalow et al., 2018). While multiplex staining with primary antibodies of the same species can be achieved using TSA-free techniques, such as those using Fab fragments (Brown et al., 2004) or antibodies of different subclasses (Ijsselsteijn et al., 2019), TSA is an attractive alternative given the added benefits of signal amplification, allowing detection of low expressed antigens.

Many commercial TSA-based multiplex IF staining kits, such as the Perkin Elmer OPAL kits, are recommended for use with a multispectral microscopy system for image acquisition and analysis. These systems capture many narrow bandwidths of light and use algorithms to separate spectral curves of multiple fluorophores. However, many research

* Corresponding author at: St John of God Subiaco Hospital, PO Box 14, Subiaco, WA 6904, Australia.
E-mail address: Tracey.lee-pullen@uwa.edu.au (T.F. Lee-Pullen).
[1] These authors contributed equally to this work.

https://doi.org/10.1016/j.jim.2019.06.011
Received 21 January 2019; Received in revised form 30 April 2019; Accepted 5 June 2019
Available online 08 June 2019
0022-1759/

groups have limited access to such systems. Traditional fluorescence detection using band pass filters can be used to distinguish multiple markers (albeit not as many) and are more widely available, but their utility for analysing multiplex IF staining is relatively unexplored. Since clinical research projects often involve assessment of large tissue areas, such as tissue microarrays (TMAs), or multiple whole tissue sections, use of a scanning system rather than a single field of view fluorescence microscope is usually preferable (Isse et al., 2012).

Here we describe our experience optimising two 5-colour immunofluorescence panels (four IF markers plus DAPI) combining TSA and indirect immunofluorescence for the assessment of tumour-infiltrating lymphocytes (TILs) in formalin-fixed, paraffin-embedded (FFPE) colorectal tissue (TMAs and whole tissue sections), for imaging on a fluorescence slide scanner with standard bandpass filters. We discuss some of the major steps and key considerations in optimising a TSA-based assay and developing multiplex assays.

2. Materials and methods

2.1. Sample preparation

The use of tissue for this work was approved by the St John of God Health Care Human Research Ethics Committee. All staining was performed using FFPE human tissue sections (4 µm thickness). Sections were dewaxed and rehydrated through graded alcohol and xylene washes. Antigen retrieval was performed in Tris-EDTA buffer (pH 9.0) using a microwave pressure cooker (Nordic Ware Microwave Tender Cooker 2.5 Quart; Amazon.com) and a microwave oven at 770 W power. The retrieval buffer was pre-heated for 8 min before boiling sections for 2 min. Endogenous peroxidase and non-specific background staining were blocked using Peroxidazed 1 and Background Sniper, respectively, (Biocare Medical, Concord, CA, USA) according to the manufacturer's instructions.

2.2. Immunofluorescence staining

For each staining panel, four antigens were immunolabelled using a combination of TSA and fluorescently-conjugated secondary antibodies. Primary antibodies used were CD4, Foxp3 (EPR6855 and 236A/E7; Abcam, Cambridge, UK), PD-L1 (E1L3N; Cell Signaling Technology, Danvers, MA, USA), PD-1 (NAT105; Cell Marque, Rocklin, CA, USA), CD8, cytokeratin (c8/144B and AE1/AE3; Agilent, Santa Clara, CA, USA), and Ki67 (SP6; ThermoFisher Scientific, Malaga, WA, Australia), all applied for 60 min at room temperature. For TSA detection, primary antibody incubation was followed by MACH 2™ HRP-Polymer (Biocare Medical) and a fluorophore-tagged TSA reagent (TSA-Cy5, TSA-FITC; Perkin Elmer, Waltham, MA, USA and TSA-AF594; ThermoFisher). Following each round, microwave treatment (as described above) was used to remove bound antibodies before proceeding to the next step. Secondary goat anti-rabbit-AF594 (Jackson ImmunoResearch Laboratories, West Grove, PA, USA) and goat anti-mouse-AF555 (Abcam), applied for 30 min, were used in place of TSA for cytokeratin and Ki67. Sections were counterstained with DAPI (Sigma, St. Louis, USA) and mounted with ProLong® Diamond Antifade mounting medium (ThermoFisher). Antibody and reagent dilutions are provided in Table 1. A flow chart of the staining protocol is provided in Suppl. Fig. 1. TMAs containing colorectal tissue, tonsil tissue and other tissue types known to express the markers of interest, such as placental tissue for PD-L1, were used as positive controls for panel optimisation. These TMAs also contained known negative control tissues for the markers of interest. All optimisation steps were performed using both positive control tissue and colorectal cancer tissue. Sections stained with matched concentrations of isotype control antibodies were included in all titration experiments. 'No primary antibody' controls were used to detect non-specific binding of secondary antibodies or TSA reagents.

2.3. Image acquisition, preparation and analysis

Images were acquired using a Pannoramic MIDI II fluorescence scanning system (3D Histech, Budapest, Hungary) equipped with an LED Spectra 6 light engine (Lumencor, Beaverton, OR, USA) and pco.edge sCMOS camera (PCO, Germany). All slides were scanned using a 20×/NA 0.8 objective (Carl Zeiss, Oberkochen, Germany), and camera settings were kept constant for intensity comparisons where appropriate. Images were prepared using CaseViewer (3D Histech), Photoshop (Adobe, San Jose, CA, USA) and StrataQuest version 6 (TissueGnostics, Vienna, Austria). Display levels are consistent where comparisons in staining intensity are made. Technical specifications, filter configurations and imaging settings are provided in Table 2, and Supplementary Tables 1 & 2. Image analysis was performed using StrataQuest version 6.

3. Results

3.1. Optimising TSA-based fluorescence IHC staining

A TSA-based assay, like chromogenic IHC, involves application of a primary antibody specific to the epitope of interest, followed by a horseradish peroxidase (HRP)-conjugated secondary. The HRP is then used to catalyse the deposition of fluorescently-labelled tyramide molecules that bind covalently to the target epitope and surrounding local area, resulting in signal amplification (Krieg and Halbhuber, 2010). These tyramide molecules remain bound to the tissue following heat or chemical treatment, which can therefore be used to strip the primary and secondary antibodies, allowing for multiple sequential rounds of staining using TSA molecules labelled with different fluorophores (Toth and Mezey, 2007; Stack et al., 2014).

One of the first steps in the development of any IHC-based assay is to determine the optimal concentration of primary antibody. The manufacturer-recommended antibody dilution for IHC in FFPE tissue was used as a guide for the starting dilution for TSA-based staining. Each antibody was titrated as a single colour stain before use in a multiplex assay. Due to the increased signal amplification of TSA detection, we found that the concentration of some primary antibodies could be decreased up to ten-fold compared to that recommended by the manufacturer, as previously reported (Gorris et al., 2018). For example, the anti-CD4 antibody we used still produced a strong specific signal at a 1:1000 dilution, with lower background staining compared to a 1:100 dilution (Fig. 1A). Increasing antibody dilutions not only saves antibody, but is also a consideration in multiplex assays to modulate signal intensity and limit spectral overlap. However, the optimal concentration for some of the antibodies used in our panels was the same as that recommended for IHC, particularly those targeting molecules showing a range of expression. Lowering the concentration of anti-PD-1 for example, resulted in loss of detection of cells expressing low levels of PD-1 (Fig. 1B). Interestingly, we also found that the staining pattern for one TSA reagent (TSA-AF594) was more punctate than that of other TSA reagents (or directly-conjugated secondary AF594) when used with the same primary antibody (Fig. 2). All primary antibodies were therefore titrated with the fluorophore that was ultimately used for its visualisation to avoid potential differences in staining pattern or intensity.

Our staining protocol was based on that recommended for the Opal™ Multiplex staining kits (Perkin Elmer) (Stack et al., 2014), but with blocking steps as previously optimised for chromogenic IHC (McCoy et al., 2015) (see Methods). Efficacy of the microwave-mediated antibody stripping was confirmed by stripping prior to adding the TSA reagent (to confirm stripping of primary/secondary antibody complexes) and by reapplying the HRP-conjugated secondary antibody, followed by a second TSA reagent after microwave stripping (to confirm stripping of any residual primary antibody) (Suppl. Fig. 2). While most primary antibodies in our panels were adequately stripped using this

Table 1
Antibody and reagent details.

Primary antibody				Secondary antibody / polymer		TSA reagent
Marker	**Clone**	**Dilution (working conc. μg/mL)**	**Step**	**Reagent**	**Dilution (working conc. μg/mL)**	**Conjugate (dilution)**
Panel 1						
CD4	EPR6855	1:1000 (0.14)	1	MACH 2 rab HRP	NA[a]	Cy5 (1:50)
Foxp3	236A/E7	1:1000 (1.00)	2	MACH 2 ms HRP	NA[a]	FITC (1:50)
Ki67	SP6	1:100 (ND)	3	Goat αrab-AF594	1:50 (30.0)	–
CK	AE1/AE3	1:50 (2.14)	3	Goat αms-AF555	1:250 (8.0)	–
DAPI	–	1:500 (10.0)	4	–	–	–
Panel 2						
PD-L1	EL13N	1:500 (1.75)	1	MACH 2 rab HRP	NA[a]	FITC (1:50)
PD-1	NAT105	1:100 (0.55)	2	MACH 2 ms HRP	NA[a]	Cy5 (1:50)
CD8	C8/144B	1:100 (1.57)	3	MACH 2 ms HRP	NA[a]	AF594 (1:100)
CK	AE1/AE3	1:50 (2.14)	4	Goat αms-AF555	1:250 (8.0)	–
DAPI	–	1:500 (10.0)	5	–	–	–

CK; cytokeratin, HRP; horseradish peroxidase, ms; mouse, NA; not applicable; ND; not determined, rab; rabbit, TSA; tyramide signal amplification
[a] Pre-diluted.

Table 2
3D Histech scanner configurations.

	Fluorophore	Excitation tranmission band[a]	Emission transmission band	Semrock filterset
Original configuration	DAPI	378–397.5 nm	412–452 nm	LED-DA/FI/TR/Cy5-A-000
	FITC	461–489 nm	497–532.5 nm	LED-DA/FI/TR/Cy5-A-000
	AF555 / Cy3	540–569 nm	577–613.5 nm	LED-DA/FI/TR/Cy5-A-000
	AF594	565–591 nm	601–682 nm	LED-mCherry-A-000
	Cy5	643.5–647 nm	657–804 nm	LED-DA/FI/TR/Cy5-A-000
Updated configuration	DAPI	378–397.5 nm	412–452 nm	LED-DA/FI/TR/Cy5-A-000
	FITC	461–489 nm	497–532.5 nm	LED-DA/FI/TR/Cy5-A-000
	AF555 / Cy3	521–547 nm	555–589 nm	SpGold-B-000
	AF594	573–594 nm	609–647 nm	SpRed-B-000
	Cy5	643.5–647 nm	657–804 nm	LED-DA/FI/TR/Cy5-A-000

[a] Resultant transmission of LED light engine and epifluorescence cube filters.

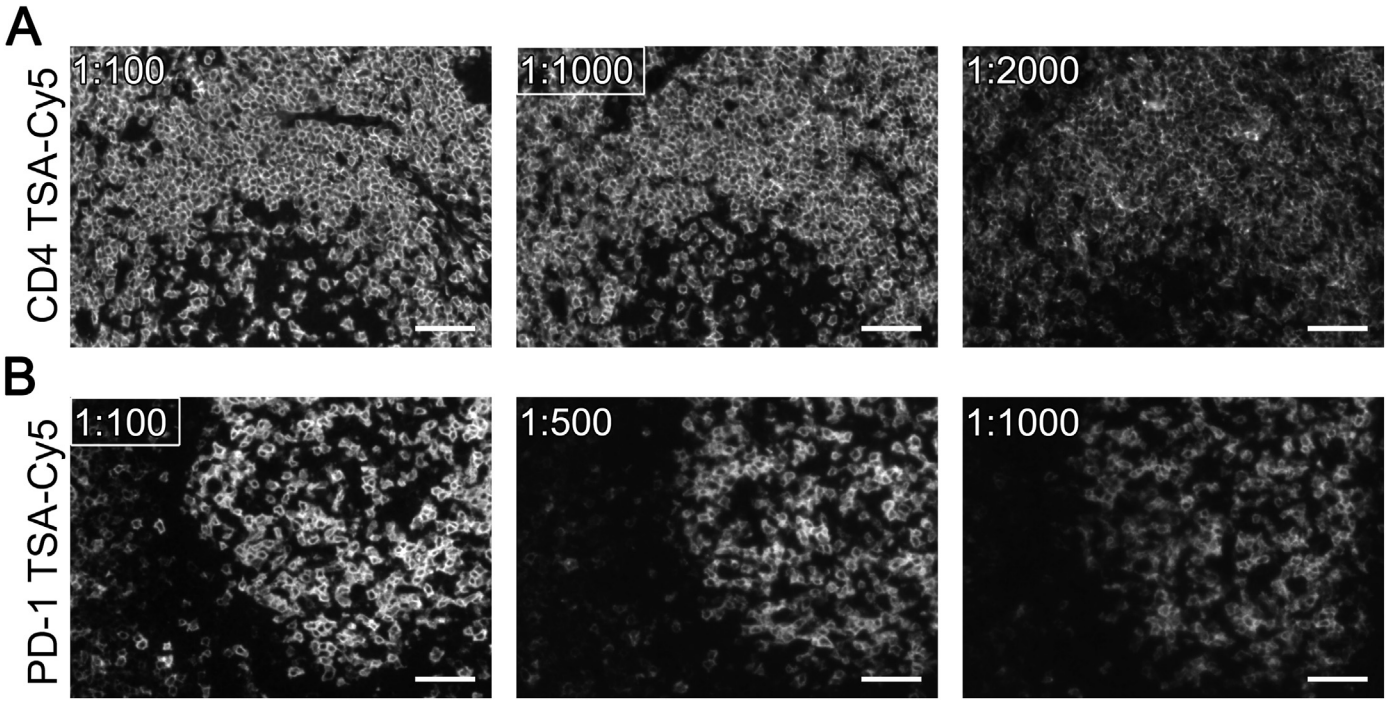

Fig. 1. Primary antibody dilution using TSA fluorescence detection. Representative images of human tonsil tissue stained with (A) anti-CD4 TSA-Cy5 and (B) anti-PD-1 TSA-Cy5 at the indicated dilutions of primary antibody. White boxes highlight dilutions selected for the multiplex assay. Image panels display grayscale captures of the same field of view from different sections of the same tonsil block. Scale bars 50 μm.

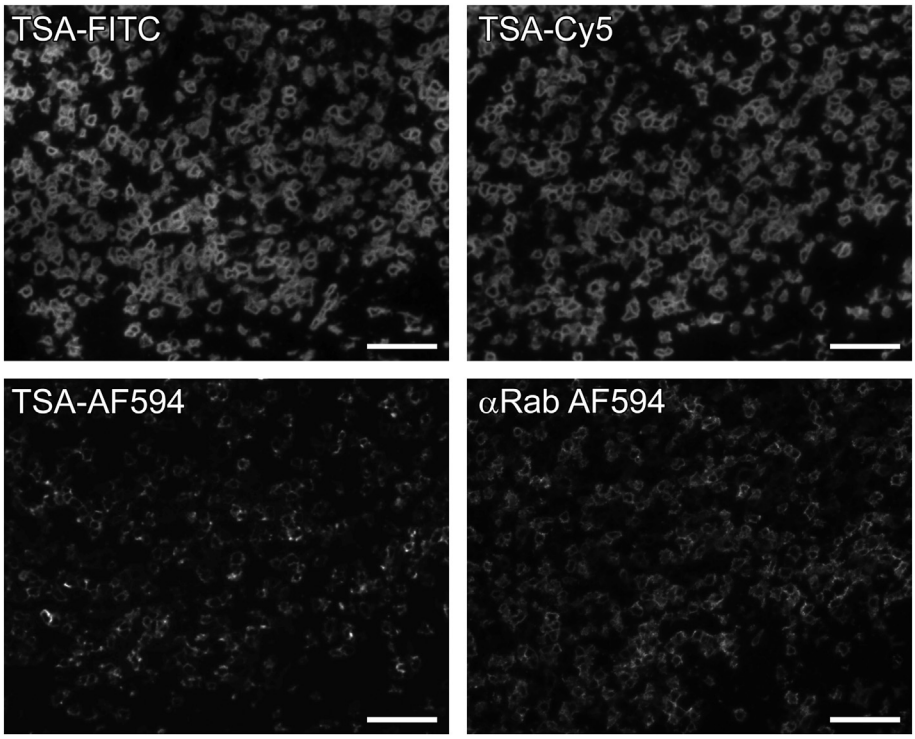

Fig. 2. Impact of detection fluorophores on primary antibody staining pattern. Representative images of human tonsil tissue stained with anti-CD4 antibody followed by TSA-FITC, TSA-Cy5, TSA-AF594 detection (using a 1:1000 dilution of primary antibody) or anti-rabbit AF594 (using a 1:50 dilution of primary antibody). Image panels display grayscale captures of the same field of view from different sections of the same tonsil block. Scale bars 50 μm.

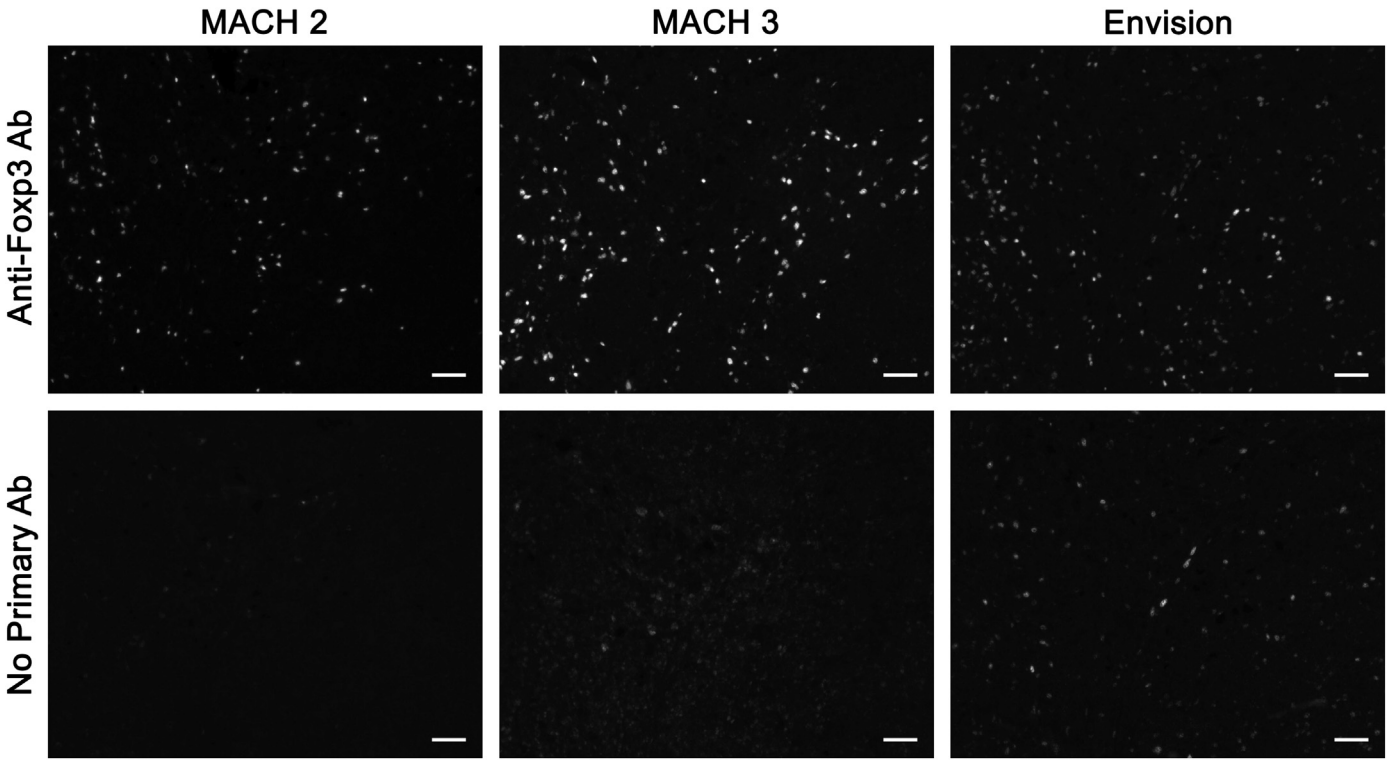

Fig. 3. Performance of different secondary detection systems in a TSA-based assay. Representative images of human colon cancer tissue labelled with anti-Foxp3 antibody (top row) or no primary antibody (bottom row), detected using the MACH 2 HRP-Polymer, MACH 3 HRP-Polymer or Envision FLEX+ detection system followed by TSA-FITC. Image panels display grayscale captures of the same field of view from different sections of the same tissue core. Display levels are consistent between detection systems, but differ between top and bottom panels (0–26,111 and 0–18,175 respectively) to best present differences in background staining. Scale bars 50 μm.

protocol, CD8 antibody was not (Suppl. Fig. 3), highlighting the need to test stripping of each antibody. To avoid cross-binding of residual CD8 antibody to successive antibodies, the staining order was adjusted to ensure PD-1 preceded CD8 staining (Suppl. Figs. 4 & 5).

When performing IHC, staining quality can vary considerably depending on the choice of secondary detection system (Anyaegbu et al., 2017). We tested three commercially available HRP-based detection systems frequently used in our IHC assays: MACH 2™ HRP and MACH

3™ HRP Polymer Detection (Biocare Medical) and Dako Envision™ FLEX + System (Agilent) in the TSA protocol. While the specific signal was comparable using each of these systems, non-specific background was increased with the MACH 3 and Envision systems (Fig. 3), most likely due to their increased sensitivity. Furthermore, overly bright staining created by increased signal amplification can accentuate fluorescence spill-over. We therefore proceeded with the optimisation process using the MACH 2 system, which had comparable background staining to the intrinsic low level of autofluorescence of the tissue (Suppl. Fig. 6).

3.2. Multiplexing with bandpass filters

As we did not have access to a multispectral imaging system, which is the recommended system for analysing multicolour images of TMAs and whole tissue sections, our aim was to develop multiplex IF assays that could be imaged using a fluorescence scanner with standard bandpass filters. This required careful panel design, for which we applied the same principles used in polychromatic flow cytometry assays, taking into account antigen expression patterns, the likelihood of co-expression and overlap in emission spectra (Baumgarth and Roederer, 2000; Perfetto et al., 2004). Modelisation tools such as Semrock's SearchLight and other online spectraviewers were useful in the initial planning of our multiplex assay, but these did not wholly replace rigorous testing of fluorophore combinations and optical configurations.

Whilst many fluorescence imaging systems are available to researchers with pre-determined configurations, it is often possible to adjust certain optical components. The fluorescence scanner available to us (Pannoramic MIDI II; 3D Histech) has six LED excitation bands (4 of which are suitable for exciting five available fluorophore reagents), and was originally equipped with three filter cubes: Quad-band (DAPI/FITC/TRITC/Cy5), CFP and mCherry (Suppl. Table 1). Based on this configuration the five fluorophores selected were DAPI, FITC, Cy3, AF594 and Cy5. We purchased a 4-colour TSA kit (Opal 4-colour fIHC Kit; Perkin Elmer), and to reduce reagent costs, combined this with a fluorescently-labelled secondary antibody.

Determining the optimal antibody-fluorophore combination and optical configuration required careful planning and optimisation. Our original design for Panel 1 produced noticeable fluorescence 'spillover' from TSA-Cy3 into AF594 due to both the inherent imbalance in intensity between a TSA- and non-TSA fluorophore, and the broad filters of the mCherry cube used (Fig. 4A). This was alleviated by replacing TSA-Cy3 with a AF555-conjugated secondary antibody (non-TSA and therefore 'dimmer' signal), however 'spill-over' from AF594 into the AF555 channel was then evident due to the increased camera exposure time required to image AF555 compared to TSA-Cy3 (Fig. 4B). To improve the separation of AF594 and AF555/Cy3 signals, the optical configuration was updated with two new bandpass filter cubes, SpGold and SpRed (narrower excitation and emission specifications) for detecting AF555/Cy3 and AF594 respectively (Table 2). While this update did not improve discrimination of TSA-Cy3 and AF594 signals (as the intensities of both fluorophores were imbalanced; Fig. 4C), it improved the discrimination of AF594 signal from the AF555 channel, producing the optimal distinction of specific signals from both channels (Fig. 4D).

While these changes to signal amplification and detection significantly reduced spill-over between most channels, they did not eliminate it completely with this scanning system configuration. For example, due to the relatively dimmer signal intensity of AF555 we have some spectral overlap from TSA-FITC into the AF555 channel. In our panels this 'cross-talk' can be managed through adjustment to the panel design (e.g. substitution of AF594 with AF555 for cytokeratin (CK) visualisation), together with spectral correction using image analysis software StrataQuest (TissueGnostics). Representative images in Fig. 5 demonstrate 'spill-over' of signal from the Foxp3+ nuclei (Fig. 5A) into the CK channel (Fig. 5B). This signal can be subtracted from the CK channel (Fig. 5C) and this corrected image is then used to create an epithelial mask based on CK staining (Fig. 5D, turquoise overlay). This type of digital correction will affect fluorescence intensity measurements and therefore consideration should be made where quantitation of antigens is required.

3.3. Final panel assessment

As staining intensity and background varies between tissue types, our tissue of interest (colorectal) was included in all optimisation experiments. Individual channels were assessed using both single stain controls and full panels to assess antibody specificity, fluorophore intensity and fluorescence spill-over.

The order of primary antibody application in multiplex IF assays has been shown to affect staining intensity (Gorris et al., 2018). Therefore each permutation of staining order for TSA assays was tested to

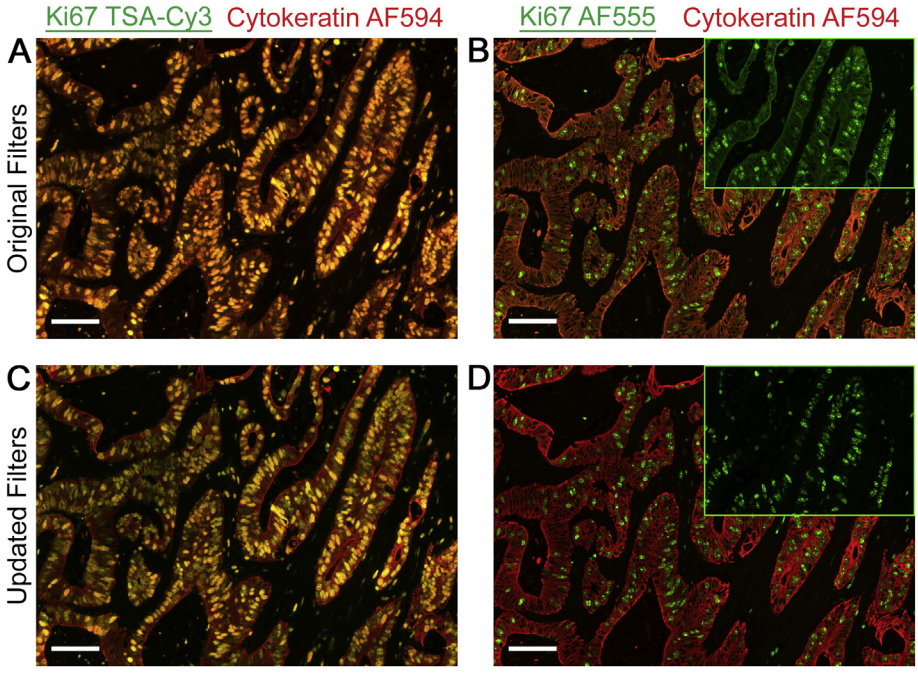

Fig. 4. Optimisation of signal intensity and optical configuration for detection of AF555 and AF594. Representative images showing the same area of human colon cancer tissue on 2 serial sections stained with cytokeratin AF594 and either Ki67 TSA-Cy3 (A and C) or Ki67 AF555 (fluorescently-labelled secondary antibody; B and D). The 2 slides were imaged using the original filter cubes (quad-band TRITC for AF555/Cy3 and mCherry for AF594; A and B) and updated narrow-bandpass filter cubes (SpGold for AF555/Cy3 and SpRed for AF594 cubes; C and D). Image panels are combined image overlays of Ki67 (green) and CK (red) channels, where yellow indicates signal present in both channels. Inset images on panels B and D show single Ki67 AF555 channel (green), illustrating 'spillover' from cytokeratin AF594 into the AF555 channel when imaged using the old optical configuration (B). Optimal distinction between these 2 channels was obtained using both updated optical filters and balanced AF555 and AF594 fluorescence intensities (D). The illumination light source for both channels was the green band of the Lumencor LED Spectra 6 light engine, with further refinement of the excitation wavelength provided by the filter cubes (Supplementary Table 1). Scale bars 50 μm.

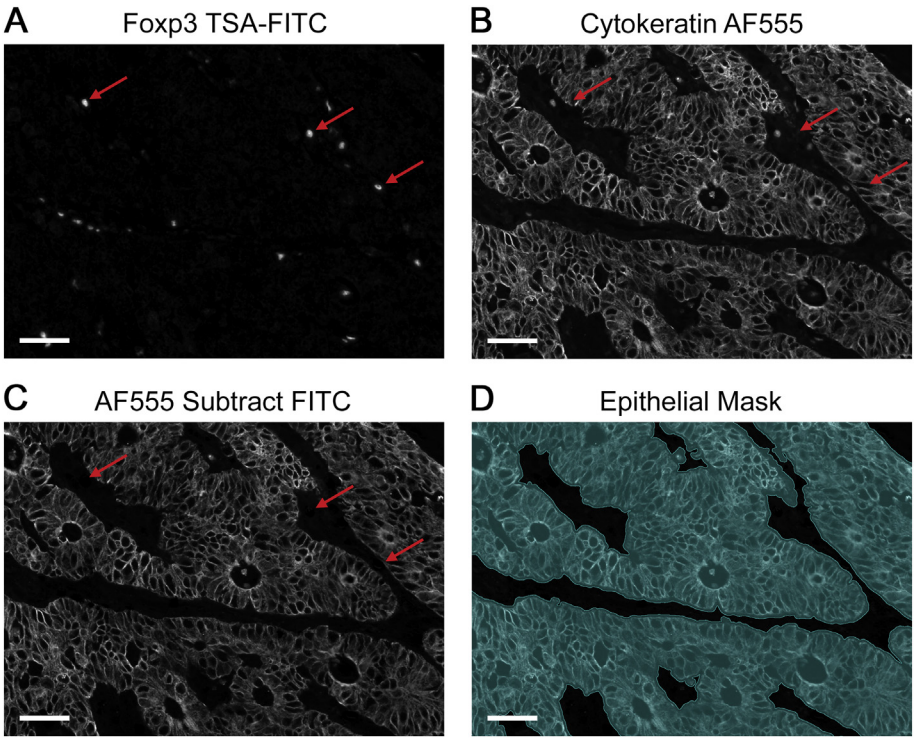

Fig. 5. Correction of spectral overlap using image analysis software. Single channel images of Foxp3 TSA-FITC (A) and Cytokeratin AF555 (B) illustrate spectral 'spillover' of FITC signal into the AF555 channel. Correction (subtraction) of FITC from AF555 (C) by StrataQuest software enables an accurate epithelial mask to be created, based on cytokeratin staining (D), turquoise overlay. All images are of the same field of view from the same tissue section (colorectal cancer). Red arrows highlight the signal from the same three Foxp3+ cells in each image. Scale bars 50 μm.

determine the optimal order for each panel (Suppl. Figs. 4 and 5). Multiple staining rounds were found to affect all antibody-TSA fluors in Panel 2, although the magnitude of this effect varies for each antibody (Suppl. Fig. 4). The staining order that performs best overall for the combined panel was selected. Importantly, staining order has a more significant effect on some antibodies, for example we found for Panel 2 that application of PD-1 antibody must precede CD8 due to ineffective stripping of the CD8 antibody complex, producing PD-1 staining at all CD8 binding sites (Suppl. Fig. 5).

Our final 5-colour panels include a combination of TSA and indirect IF to give satisfactory discrimination between antigens (Table 1 and Fig. 6), and negligible tissue autofluorescence (Suppl. Fig. 7). This combination of staining methods produces optimal fluorescent signal intensities for the resolution of five fluorophores using a non-spectral, fluorescence scanning microscope. Furthermore, it also reduces the number of stripping steps, reducing the length of the protocol. This differs from the use of a spectral imaging system where uniform emission signals (e.g. all TSA fluorophores) are recommended (Stack et al., 2014).

To realise the full utility of multiplex staining, a robust and accurate quantitation method is required. These staining panels were designed to enable assessment of immune cell density and spatial distribution in human colorectal cancer samples. Using StrataQuest image analysis software, we are using these panels to quantitate single-, double- and triple-positive cells infiltrating the tumour and in the surrounding stroma in tissue microarrays (TMAs) and biopsy sections (Fig. 7 and Suppl. Fig. 8).

4. Discussion

TSA-based multiplex IF offers several advantages over traditional chromogenic IHC, including the ability to detect multiple markers on the same tissue section, without the requirement for primary antibodies to be raised in different species, and to detect co-localisation of proteins in the same cellular compartment. Most commercial TSA-based multiplex IF kits are recommended for use with a multispectral imaging and analysis system due to their ability to accurately resolve multiple spectral signatures and exclude tissue autofluorescence. However, we have demonstrated that TSA-based multiplexing can also be achieved by adapting the staining protocol, and imaging with a non-spectral fluorescence scanning systems equipped with narrow band-pass filters. Development of a multiplex IF staining panel using TSA requires precise planning, panel design and optimisation. However, the time invested is offset by the gain of multi-parametric information (four biological markers versus one for the panels described), enabling more detailed investigation of complex cellular interactions and biological processes.

Thorough validation of primary antibody staining is critical to the successful development of any IHC-based assay, including multiplex IF assays. Demonstration of antibody specificity requires the use of appropriate controls, such as tissues or cell lines known not to express the protein of interest, in addition to including sections stained with no primary antibody or an isotype control (Goldstein et al., 2007; Bordeaux et al., 2010; Hewitt et al., 2014; Manuel et al., 2018). In developing our protocols, we used antibodies we had previously validated for use in chromogenic IHC. Antibodies to lymphocyte markers and cytokeratin were assessed using tissue known to contain varying degrees of immune infiltrate and no epithelial tissue, respectively. The anti-PD-L1 antibody was evaluated using IHC reference standard slides consisting of cell lines with defined negative, low, intermediate or strong expression of PD-L1 (Anyaegbu et al., 2017). It is also important to consider other factors that may influence staining quality and/or antibody specificity, when validating a new antibody, such as antibody batch variation and tissue fixation and storage (Goldstein et al., 2007; Shi et al., 2007; Bordeaux et al., 2010).

Due to the increased signal amplification of the TSA-conjugated fluorophores, we found that some primary antibody concentrations could be reduced by 10-fold compared to the manufacturer-recommended dilution for IHC. In addition, high level amplification systems were not required with the TSA protocols. In fact, in our hands, use of the MACH-3 or Envision systems resulted in substantial non-specific background, whereas the MACH-2 system provided the optimal balance between specificity & sensitivity when using TSA-conjugated fluorophores. One approach to reduce non-specific staining produced by secondary detection systems would be to reduce the concentration of

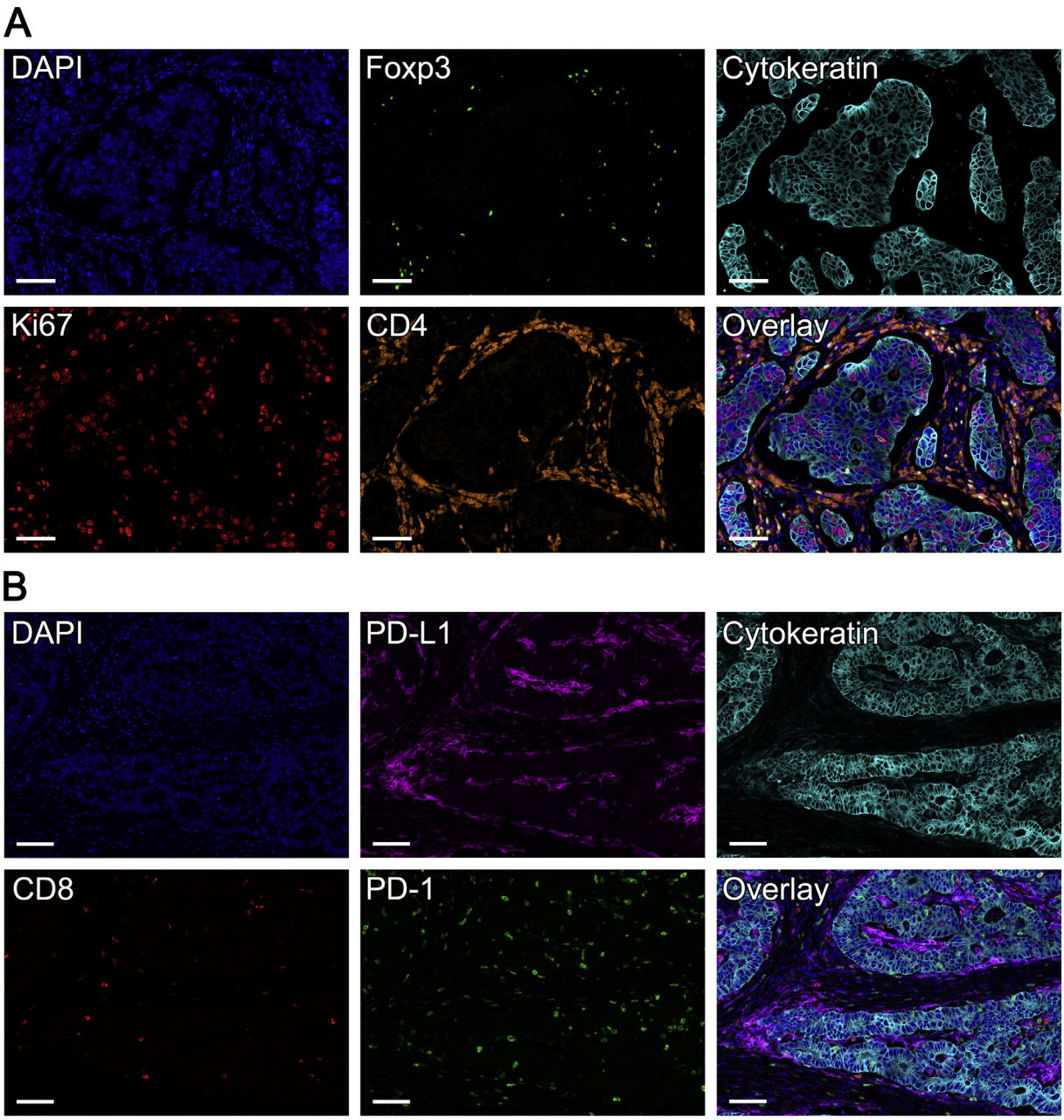

Fig. 6. Optimised 5-colour panels. Representative images of human colon cancer tissue showing each individual channel and 5-colour overlay of all channels in (A) Panel 1 and (B) Panel 2. A full list of antibodies and fluorophores are provided in Table 1. Scale bars 50 μm.

secondary antibody and/or detection reagent. However, this can often be difficult to accomplish when using detection kits that include pre-dilute reagents. In our hands, reducing the TSA application time did not significantly impact signal intensity (data not shown).

TSA protocols offer a good method for dealing with cross-binding of antibodies raised in the same species, however, as with many protocols, each component needs to be carefully tested. Differences in both stripping efficacy and the order of antibody application in TSA-based multiplex assays can significantly impact assay performance, as previously reported (Gorris et al., 2018) and as we found for our second panel (Suppl. Figs. 3–5). TSA fluorophore intensity can be affected by both preceding steps and subsequent staining rounds. Antibody binding can potentially be reduced by the effect of additional heat or chemical treatment steps on epitope availability, and by interference of previously-bound TSA fluorophore complexes. More apparent in our study is a reduction in fluorescence intensity after multiple rounds of staining, likely due to removal of bound TSA fluorophores with repeated rounds of microwave treatments (Stack et al., 2014). Staining order can also be important for specific antibody combinations such as PD-1 and CD8 in Panel 2. PD-1 staining after CD8 results in apparent co-labelling of all CD8+ cells with the PD-1 detection fluorophore (TSA-Cy5). This is evident, both as PD-1 signal at all anti-CD8 binding sites (Suppl. Fig. 5), most likely due to incomplete stripping of the anti-CD8 antibody complex and subsequent binding with the next round of TSA fluorophore (Cy5; Suppl. Fig. 3B). The reduced intensity of CD8 TSA-AF594 (Suppl. Fig. 3B, iii) compared to the single stain (Suppl. Fig. 3A, iii), together with increased TSA-Cy5 signal (Suppl. Fig. 3B, vi) indicate FRET is occurring, where emitted light from TSA-AF594 is exciting the closely bound TSA-Cy5. These findings highlight the importance of confirming stripping efficacy of all antibodies, and also demonstrates the importance of assessing each marker in the combined multiplex panel to determine the optimal staining order.

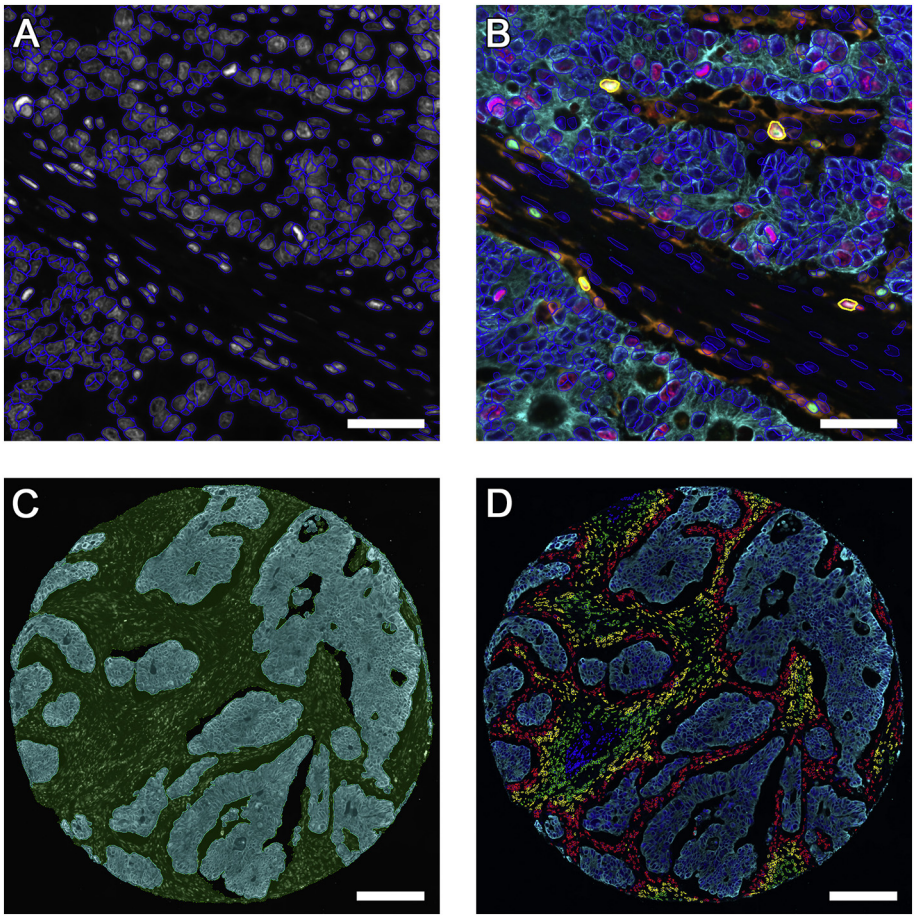

Fig. 7. Quantitative analysis of 5-colour multiplex immunofluorescence images of a colorectal cancer tissue core using StrataQuest software. (A) Nuclear segmentation overlaid on DAPI channel. (B) Nuclear segmentation overlayed on all channel image. Triple positive proliferating regulatory T cells (CD4+ Foxp3+ Ki67+) are selected in the software and highlighted with yellow outline. Scale Bars: 50 μm. (C) TMA core (colorectal tumour tissue) overlayed with area masks for epithelium (turquoise) and stroma (green) generated by detection of tissue and cytokeratin. (D) Spatial detection of cell nuclei at different distances from the epithelial mask (red within 25 μm, yellow 25–50 μm, green 50–100 μm, blue > 100 μm). Scale bars: 200 μm.

Image collection and visualisation settings are also important considerations when optimising IF protocols. Filters, camera exposure times, and image display levels must be kept consistent when comparing samples. Camera exposure times should be set using the brightest stained sample for each channel to ensure saturation is not reached. Many commercial image viewers will automatically adjust the displayed levels to optimise image visualisation. Care should therefore be taken to ensure displayed levels are consistent between samples when comparing staining intensity, especially when using more sensitive 16-bit CCD cameras.

Data handling and image analysis are important considerations for multiplex IHC experiments. Whole-slide fluorescence scanning can produce large data files, requiring both appropriate software, able to display and analyse data, together with the computing power to do so. Whilst most scanning systems have associated software platforms able to view such data sets, the market for detailed analysis platforms is growing. The StrataQuest analysis software utilised by our research group is customisable to a wide range of image analysis applications and is able to handle data files from a range of imaging systems. This allows us to realise the full potential of our optimised 5-colour assay.

The light source available for fluorescence excitation and range of commercially available TSA reagents informed the choice of fluorophores for our assays. Increased flexibility to both of these constraints could be of significant benefit to multiplex IHC assays by increasing the number of parameters that can be studied simultaneously and reducing spectral cross-talk (Prost et al., 2016). A sound understanding of the fluorophores selected and the optical configuration of our imaging system informed selection of the most appropriate antibody-fluorophore combinations, minimising subsequent panel rearrangements and avoiding titrating each antibody with multiple fluorophores. We found the use of freely available online spectral viewers of great value in predicting fluorophore signal collection and limiting spectral spillover using standard bandpass filter microscopes. Spectral viewers, such as the Semrock SearchLight Spectra Viewer, can provide important additional information when assessing optical configuration specifications, as components such as filters and dichroic mirrors often have transition zones that are better visualised in conjunction with fluorophore excitation and emission profiles. Although these tools can be useful for predicting spectral overlap between fluorophores using system-specific optical configurations, they are not absolutely accurate.

Our scanning system was originally configured with 2 filter cubes with the hope we could resolve 5 fluorophores with minimal switching of the filter cubes. However as we and others (Zhang et al., 2017) have found, resolution of closely related spectral emissions requires narrow bandpass filters when using a non-spectral scanner. The trade-off to improved discrimination of fluorophores using multiple filters is an increase to scanning time (due to physical switching of the filter cubes). In addition, careful assessment of optical alignment is required to ensure the focus (z-plane) and x, y image co-registrations are accurate between filter cubes. Whilst we were unable to eliminate spectral spillover using bandpass filter configuration alone, by adjusting the panel design (antibody-fluorophore assignment) and using spectral corrections in analysis software, we were able to mitigate potential issues in quantifying antigen expression. These types of software corrections can be performed in freeware such as ImageJ, as well as in digital image analysis software packages that provide a quantitative high throughput analysis pipeline. Image manipulations such as these 'subtractions' differ from compensation algorithms employed in flow cytometry analysis packages and spectral unmixing, and care should be taken in utilising these tools where quantitation of fluorescence intensity is required. In our panels, the software correction is made in a channel used solely to create a digital 'mask', and, importantly, not to quantify

fluorescence intensity.

In summary, we successfully optimised two 5-colour immunofluorescence panels, which can be imaged using a fluorescence scanner with standard bandpass filters, or a standard epifluorescence microscope. Theoretically six parameters could be achieved by substituting the light engine to include a far-red excitation line. Whilst this approach has its limitations compared to a multispectral system, including a lower limit to the number of markers that can be simultaneously detected (currently 8-parameters using multispectral detection; Gorris et al., 2018), the level of information gained is considerably increased when compared to chromogenic IHC. An additional reported benefit of multispectral imaging is the isolation of tissue autofluorescence (a recognised issue for immunofluorescence assays; Mansfield, 2017). Fortunately, the levels of autofluorescence observed in our imaging is negligible (Suppl. Fig. 7), mostly due to the amplified signal using TSA staining and subsequent short camera exposure times for imaging. This results in accurate distinction and quantitation of staining from tissue autofluorescence for all channels. We are now using these panels, together with quantitative analysis software, to interrogate the local anti-tumour immune response in patients undergoing treatment for colorectal cancer by high throughput scanning and analysis of large tissue microarrays and biopsy fragments.

Competing interests

The authors declare no competing interests.

Acknowledgements

The authors would like to thank Raelene Endersby of the Telethon Kids Institute for facilitating access to the fluorescence scanning system, Paul Rigby and Alysia Hubbard of the Centre for Microscopy, Characterisation and Analysis at the University of Western Australia (a facility funded by the University and the State and Commonwealth Governments), and Brad Hope of Coherent Scientific, for their valuable advice and assistance.

Funding

This work was funded by the Tonkinson Colorectal Cancer Research Fund. The fluorescence scanning system was purchased for Telethon Kids Institute with funding from Bright Blue – The Police Commissioner's Fund for Sick Kids. StrataQuest image analysis software was funded by the Tonkinson Colorectal Cancer Research Fund and the St John of God Foundation.

Appendix A. Supplementary data

Supplementary data to this article can be found online at https://doi.org/10.1016/j.jim.2019.06.011.

References

Anyaegbu, C.C., Garrett, K., Hemmings, C., Lee-Pullen, T.F., McCoy, M.J., 2017. Immunohistochemical detection of PD-L1 for research studies: which antibody and what protocol? Pathology 49, 427–430.

Baumgarth, N., Roederer, M., 2000. A practical approach to multicolor flow cytometry for immunophenotyping. J. Immunol. Methods 243, 77–97.

Blom, S., Paavolainen, L., Bychkov, D., Turkki, R., Maki-Teeri, P., Hemmes, A., Valimaki, K., Lundin, J., Kallioniemi, O., Pellinen, T., 2017. Systems pathology by multiplexed immunohistochemistry and whole-slide digital image analysis. Sci. Rep. 7, 15580.

Bordeaux, J., Welsh, A., Agarwal, S., Killiam, E., Baquero, M., Hanna, J., Anagnostou, V., Rimm, D., 2010. Antibody validation. Biotechniques 48, 197–209.

Brown, J.K., Pemberton, A.D., Wright, S.H., Miller, H.R., 2004. Primary antibody-fab fragment complexes: a flexible alternative to traditional direct and indirect immunolabeling techniques. J. Histochem. Cytochem. 52 (1219–30).

Buchwalow, I., Samoilova, V., Boecker, W., Tiemann, M., 2018. Multiple immunolabeling with antibodies from the same host species in combination with tyramide signal amplification. Acta Histochem. 120, 405–411.

Feng, Z., Bethmann, D., Kappler, M., Ballesteros-Merino, C., Eckert, A., Bell, R.B., Cheng, A., Bui, T., Leidner, R., Urba, W.J., Johnson, K., Hoyt, C., Bifulco, C.B., Bukur, J., Wickenhauser, C., Seliger, B., Fox, B.A., 2017. Multiparametric immune profiling in HPV- oral squamous cell cancer. JCI Insight 2.

Galon, J., Mlecnik, B., Bindea, G., Angell, H.K., Berger, A., Lagorce, C., Lugli, A., Zlobec, I., Hartmann, A., Bifulco, C., Nagtegaal, I.D., Palmqvist, R., Masucci, G.V., Botti, G., Tatangelo, F., Delrio, P., Maio, M., Laghi, L., Grizzi, F., Asslaber, M., D'Arrigo, C., Vidal-Vanaclocha, F., Zavadova, E., Chouchane, L., Ohashi, P.S., Hafezi-Bakhtiari, S., Wouters, B.G., Roehrl, M., Nguyen, L., Kawakami, Y., Hazama, S., Okuno, K., Ogino, S., Gibbs, P., Waring, P., Sato, N., Torigoe, T., Itoh, K., Patel, P.S., Shukla, S.N., Wang, Y., Kopetz, S., Sinicrope, F.A., Scripcariu, V., Ascierto, P.A., Marincola, F.M., Fox, B.A., Pages, F., 2014. Towards the introduction of the 'Immunoscore' in the classification of malignant tumours. J. Pathol. 232, 199–209.

Goldstein, N.S., Hewitt, S.M., Taylor, C.R., Yaziji, H., Hicks, D.G., Members of Ad-Hoc Committee On Immunohistochemistry, S, 2007. Recommendations for improved standardization of immunohistochemistry. Appl. Immunohistochem. Mol. Morphol. 15 (124–33).

Gorris, M.A.J., Halilovic, A., Rabold, K., van Duffelen, A., Wickramasinghe, I.N., Verweij, D., Wortel, I.M.N., Textor, J.C., de Vries, I.J.M., Figdor, C.G., 2018. Eight-color multiplex immunohistochemistry for simultaneous detection of multiple immune checkpoint molecules within the tumor microenvironment. J. Immunol. 200, 347–354.

Hewitt, S.M., Baskin, D.G., Frevert, C.W., Stahl, W.L., Rosa-Molinar, E., 2014. Controls for immunohistochemistry: the histochemical Society's standards of practice for validation of immunohistochemical assays. J. Histochem. Cytochem. 62 (693–7).

Ijsselsteijn, M.E., Brouwer, T.P., Abdulrahman, Z., Reidy, E., Ramalheiro, A., Heeren, A.M., Vahrmeijer, A., Jordanova, E.S., de Miranda, N.F., 2019. Cancer immunophenotyping by seven-colour multispectral imaging without tyramide signal amplification. J Pathol Clin Res 5, 3–11.

Isse, K., Lesniak, A., Grama, K., Roysam, B., Minervini, M.I., Demetris, A.J., 2012. Digital transplantation pathology: combining whole slide imaging, multiplex staining and automated image analysis. Am. J. Transplant. 12, 27–37.

Krieg, R., Halbhuber, K.J., 2010. Detection of endogenous and immuno-bound peroxidase–the status quo in histochemistry. Prog. Histochem. Cytochem. 45, 81–139.

Mansfield, J.R., 2017. Phenotyping multiple subsets of immune cells in situ in FFPE tissue sections: an overview of methodologies. Methods Mol. Biol. 1546, 75–99.

Manuel, S.L., Johnson, B.W., Frevert, C.W., Duncan, F.E., 2018. Revisiting the scientific method to improve rigor and reproducibility of immunohistochemistry in reproductive science. Biol. Reprod. 99 (4), 673–677.

McCoy, M.J., Hemmings, C., Miller, T.J., Austin, S.J., Bulsara, M.K., Zeps, N., Nowak, A.K., Lake, R.A., Platell, C.F., 2015. Low stromal Foxp3+ regulatory T-cell density is associated with complete response to neoadjuvant chemoradiotherapy in rectal cancer. Br. J. Cancer 113 (1677–86).

Mlecnik, B., Tosolini, M., Kirilovsky, A., Berger, A., Bindea, G., Meatchi, T., Bruneval, P., Trajanoski, Z., Fridman, W.H., Pages, F., Galon, J., 2011. Histopathologic-based prognostic factors of colorectal cancers are associated with the state of the local immune reaction. J. Clin. Oncol. 29 (610–8).

Pages, F., Mlecnik, B., Marliot, F., Bindea, G., Ou, F.S., Bifulco, C., Lugli, A., Zlobec, I., Rau, T.T., Berger, M.D., Nagtegaal, I.D., Vink-Borger, E., Hartmann, A., Geppert, C., Kolwelter, J., Merkel, S., Grutzmann, R., Van den Eynde, M., Jouret-Mourin, A., Kartheuser, A., Leonard, D., Remue, C., Wang, J.Y., Bavi, P., Roehrl, M.H.A., Ohashi, P.S., Nguyen, L.T., Han, S., MacGregor, H.L., Hafezi-Bakhtiari, S., Wouters, B.G., Masucci, G.V., Andersson, E.K., Zavadova, E., Vocka, M., Spacek, J., Petruzelka, L., Konopasek, B., Dundr, P., Skalova, H., Nemejcova, K., Botti, G., Tatangelo, F., Delrio, P., Ciliberto, G., Maio, M., Laghi, L., Grizzi, F., Fredriksen, T., Buttard, B., Angelova, M., Vasaturo, A., Maby, P., Church, S.E., Angell, H.K., Lafontaine, L., Bruni, D., El Sissy, C., Haicheur, N., Kirilovsky, A., Berger, A., Lagorce, C., Meyers, J.P., Paustian, C., Feng, Z., Ballesteros-Merino, C., Dijkstra, J., Van de Water, C., Van Lent-van Vliet, S., Knijn, N., Musina, A.M., Scripcariu, D.V., Popivanova, B., Xu, M., Fujita, T., Hazama, S., Suzuki, N., Nagano, H., Okuno, K., Torigoe, T., Sato, N., Furuhata, T., Takemasa, I., Itoh, K., Patel, P.S., Vora, H.H., Shah, B., Patel, J.B., Rajvik, K.N., Pandya, S.J., Shukla, S.N., Wang, Y., Zhang, G., Kawakami, Y., Marincola, F.M., Ascierto, P.A., Sargent, D.J., Fox, B.A., Galon, J., 2018. International validation of the consensus Immunoscore for the classification of colon cancer: a prognostic and accuracy study. Lancet 391, 2128–2139.

Parra, E.R., Uraoka, N., Jiang, M., Cook, P., Gibbons, D., Forget, M.A., Bernatchez, C., Haymaker, C., Wistuba, I.I., Rodriguez-Canales, J., 2017. Validation of multiplex immunofluorescence panels using multispectral microscopy for immune-profiling of formalin-fixed and paraffin-embedded human tumor tissues. Sci. Rep. 7, 13380.

Parra, E.R., Francisco-Cruz, A., Wistuba, I.I., 2019. State-of-the-art of profiling immune contexture in the era of multiplexed staining and digital analysis to study paraffin tumor tissues. Cancers (Basel) 11.

Perfetto, S.P., Chattopadhyay, P.K., Roederer, M., 2004. Seventeen-colour flow cytometry: unravelling the immune system. Nat. Rev. Immunol. 4 (648–55).

Prost, S., Kishen, R.E., Kluth, D.C., Bellamy, C.O., 2016. Choice of illumination system & fluorophore for multiplex immunofluorescence on FFPE tissue sections. PLoS One 11, e0162419.

Schnell, A., Schmidl, C., Herr, W., Siska, P.J., 2018. The peripheral and Intratumoral immune cell landscape in Cancer patients: a proxy for tumor biology and a tool for outcome prediction. Biomedicines 6.

Shi, S.R., Liu, C., Taylor, C.R., 2007. Standardization of immunohistochemistry for formalin-fixed, paraffin-embedded tissue sections based on the antigen-retrieval technique: from experiments to hypothesis. J. Histochem. Cytochem. 55 (105–9).

Stack, E.C., Wang, C., Roman, K.A., Hoyt, C.C., 2014. Multiplexed immunohistochemistry, imaging, and quantitation: a review, with an assessment of Tyramide signal amplification, multispectral imaging and multiplex analysis.

Methods 70, 46–58.
Toth, Z.E., Mezey, E., 2007. Simultaneous visualization of multiple antigens with tyramide signal amplification using antibodies from the same species. J. Histochem. Cytochem. 55 (545–54).
van der Loos, C.M., 2008. Multiple immunoenzyme staining: methods and visualizations for the observation with spectral imaging. J. Histochem. Cytochem. 56 (313–28).
Zhang, W., Hubbard, A., Jones, T., Racolta, A., Bhaumik, S., Cummins, N., Zhang, L., Garsha, K., Ventura, F., Lefever, M.R., Lu, Z., Hurley, J.K., Day, W.A., Pestic-Dragovich, L., Morrison, L.E., Tang, L., 2017. Fully automated 5-plex fluorescent immunohistochemistry with tyramide signal amplification and same species antibodies. Lab. Investig. 97, 873–885.